

Cooling and Solidification of Melted Drops in an Immiscible Cooling Medium

By Yuan-Zhou Xi, Ting-Jie Wang*, Xin Li, and Yong Jin

The cooling and solidification of melted drops during their movement in an immiscible cooling medium is widely employed for granulation in the chemical industry, and a study of these processes provides a basis for the design of the granulation tower height and the temperature of the cooling medium is reported. A physical model of the cooling and solidification of the drop is established and the numerical calculation is performed. The influences of the key factors in the solidification, i.e., Bi number, drop diameter, temperature of the cooling medium, etc. are presented. The cooling and solidification during wax granulation in a water-cooling tower and during urea granulation in an air-cooling tower (spraying tower) are described in detail. Characteristics of the solidification and temperature distribution within the particle at different times are shown. The model and calculations can be used for structure design of the granulation tower and optimization of the operation parameters.

1 Introduction

The granulation method of drop formation and solidification of the melted material in an immiscible cooling medium is widely used in chemical engineering, e.g., urea granulation in an air-cooling tower (spraying tower), some fertilizer granulations in an oil-cooling tower, and spherical wax granulation in a water-cooling tower [1]. In the granulation process in air-cooling towers and oil-cooling towers the melted material is sprayed by a sprayer to form a series of drops in the tower. The drops contract to spheres due to the interfacial tension between the drop and the cooling medium. After a short period of acceleration, the drops reach a terminal velocity and settle down freely. During the settling period, convective heat transfer from the drops to the cooling medium causes the drops to gradually solidify into solid particles. Wax granulation in a water-cooling tower is another new method that makes use of the insolubility of wax and water. Melted wax drops are squeezed out from the nozzles and contract to spheres in the granulation holes at the bottom of the granulation tower. Since the density of wax is lower than water, the wax drops move upward in the tower due to buoyancy. During the rising process of the drops, heat transfer from the drops to the cooling water causes the melted wax drops to gradually solidify. The particles are discharged by the circulatory overflow at the top of the tower and re-cooled in a chute by spraying cool water. After dehydration, spherical wax particles are obtained [1].

The structure design and the temperature setting of the cooling medium in the three granulation technologies above depend on the characteristics of the movement and solidification of the drops. During solidification, the solid-liquid interface moves from the drop surface to the drop center. The key in the analysis of drop solidification is the tracking

of the time-varying phase front. Due to the non-linear characteristics of the phase front, analytic solutions exist only for one-dimensional cases of an infinite or semi-infinite region with simple initial and boundary conditions and constant thermal properties [2]. This paper focuses on the process of drop solidification in the cooling medium and its physical model. A variable time-step method based on the control volume method [3] is employed to track the phase front. The time-varying phase front and the temperature distribution within the drop are calculated. These results can be used as the basis for granulation tower design and the optimization of operation parameters.

2 Heat Transfer between Particles and the Cooling Medium

2.1 Movement of the Particles

A particle rises or settles freely in the granulation tower. The terminal velocity of the particle depends on the physical properties of the particle and the cooling medium. The residence time of the particle in the tower mainly depends on the particle velocity and the height of the tower.

In the granulation tower, drops form through the distributor or sprayer. After a short period of acceleration, the drop reaches its terminal velocity, and in this state the composite force acting on the particle is equal to zero. The terminal velocity of the particle can be calculated from the force equilibrium equation.

In the case of wax granulation, when a wax particle reaches its terminal velocity, the buoyancy, gravity, and drag forces acting on the particle reach equilibrium¹⁾:

$$F_B - F_g - F_D = 0 \quad (1)$$

[*] Y.-Z. Xi, T.-J. Wang (wangtj@mail.tsinghua.edu.cn), X. Li, Y. Jin, Department of Chemical Engineering, Tsinghua University, Beijing 100084, China.

1) List of symbols at the end of the paper.

In the case of urea granulation in an air-cooling tower, the buoyancy due to air can be neglected, and the gravity and drag force acting on the particle are balanced when the terminal velocity is reached:

$$F_g - F_D = 0 \quad (2)$$

where $F_b = \frac{1}{6}\pi d^3 \rho_c g$, $F_g = \frac{1}{6}\pi d^3 \rho_d g$, $F_D = \xi A_p \frac{\rho_c u^2}{2}$, $A_p = \pi d^2/4$. When the particle movement is in a turbulent flow regime ($Re > 1000$), $\xi = 0.44$. When the particle movement is in a transition regime between turbulent flow and laminar flow ($0.1 < Re < 1000$) [4]: $\xi = \left(\frac{24}{Re}\right) \left(1 + 0.14Re^{0.70}\right)$, where $Re = \frac{d u_p \rho_c}{\mu_c}$.

2.2 Convective Heat Transfer between the Particle and Cooling Medium

The convective heat transfer coefficient between the particle and the cooling medium depends on the relative movement between the particle and the cooling medium and the physical properties of the cooling medium. The Nu number, which is related to the heat transfer coefficient, has the following dimensionless correlation [6]:

$$Nu = 2.0 + b Pr^{1/3} Re^{1/2} \quad (3)$$

where $Nu = \frac{hd}{k_c}$, $Pr = \frac{C_p \mu_c}{k_c}$. The constant $b = 0.79$ when the cooling medium is water. The constant $b = 0.69$ when the cooling medium is air.

3 Physical Model of Drop Solidification

Wax granulation in a water-cooling tower and urea granulation in an air-cooling tower have the same following characteristics: (1) The drop of melted material forms in the cooling medium through a distributor or a sprayer; (2) The drop contracts to a spherical shape under the force of interfacial tension; (3) The drop accelerates to a terminal velocity in a short time and rises up or settles down freely; (4) During the movement of the drop in the tower, heat transfer occurs from the drop to the cooling medium and the drop is solidified into a particle.

Drop solidification in the tower mainly depends on the physical properties of the drop and cooling medium and the relative movement between the two phases, such as the initial temperature of the drop, drop diameter, temperature of the cooling medium, and the heat transfer coefficient. In order to simplify the physical model of drop solidification, some reasonable assumptions are made as follows: (1) The drop forms and keeps an ideal spherical shape under the force of interfacial tension during rising or settling, and there is no circulatory flow within the drop. (2) The drop solidifies at a fixed temperature (the freezing-point) and there is a liquid-solid interface between the solid phase and liquid phase.

(3) The density of the particle can be assumed constant, and is given by the average density of the solid and liquid state. (4) The temperature of the melted material is taken as the initial temperature in the drop solidification process. The average temperature of the cooling medium in the tower is taken as the temperature of the cooling medium. (5) Heat capacity and thermal conductivity are specified as constant. The convective heat transfer coefficient around the drop is calculated from Eq. (3); (6) The brief period of drop acceleration can be neglected.

3.1 Theoretical Model

A drop at an initial temperature T_o ($T_o > T_f$, T_f denotes the freezing-point temperature) is cooled in the cooling medium at temperature T_∞ ($T_\infty < T_f$), and the convective heat transfer coefficient is h . The whole solidification process can be divided into two stages. In the first stage (cooling stage), the drop temperature decreases until the surface temperature has decreased to its freezing-point. During this stage no phase change occurs. This is a heat conduction process of a spherical drop with the third boundary condition. The time for the first stage is t_f . In the second stage (solidification stage), phase change occurs from the exterior surface of the drop and the solid-liquid interface moves toward the drop center as time proceeds. When the solid-liquid interface reaches the drop center, the solidification stage is completed. A schematic diagram of this stage is shown in Fig. 1.

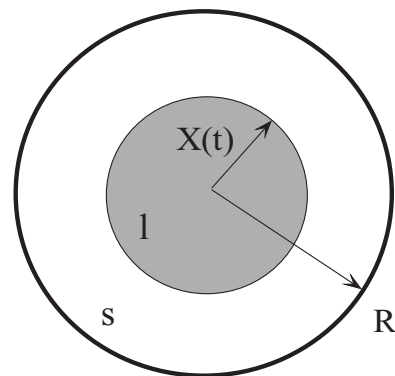


Figure 1. Schematic of the solidification of a spherical drop.

To simplify the process equation, non-dimensional variables are introduced as follows:

Non-dimensional temperature: $\varphi = \frac{C_s(T - T_f)}{L}$

Non-dimensional time: $\tau = \frac{k_s}{\rho_d C_s R^2} t$

Non-dimensional coordinate: $\eta = \frac{r}{R}$

Non-dimensional position of solid-liquid interface: $\chi = \frac{X}{R}$

Bi number: $Bi = \frac{hR}{k_s}$

According to above definition of the non-dimensional temperature, $\varphi = 0$ when the temperature is at the freezing-

point; $\varphi > 0$ when the temperature is above the freezing-point, and $\varphi < 0$ when the temperature is below the freezing-point. The equations of the two stages can be expressed as follows:

In the first stage (cooling stage):

$$\frac{\partial \varphi}{\partial \tau} = \frac{\alpha_l}{\alpha_s} \frac{1}{\eta^2} \frac{\partial}{\partial \eta} \left(\eta^2 \frac{\partial \varphi}{\partial \eta} \right) \quad 0 < \eta < 1, \quad 0 < \tau < \tau_f \quad (4)$$

Initial condition: $\varphi(\eta, 0) = \varphi_0 \quad 0 \leq \eta \leq 1$

Boundary conditions:

$$(1) \left. \frac{\partial \varphi}{\partial \eta} \right|_{\eta=0} = 0 \quad 0 \leq \tau \leq \tau_f$$

$$(2) - \left. \frac{\partial \varphi}{\partial \eta} \right|_{\eta=1} = \frac{k_s}{k_l} \text{Bi}(\varphi - \varphi_\infty) \quad 0 \leq \tau \leq \tau_f$$

In the second stage (solidification stage):

In the liquid region:

$$\frac{\partial \varphi}{\partial \tau} = \frac{\alpha_l}{\alpha_s} \frac{1}{\eta^2} \frac{\partial}{\partial \eta} \left(\eta^2 \frac{\partial \varphi}{\partial \eta} \right) \quad 0 < \eta < \chi(\tau), \quad \tau > \tau_f \quad (5a)$$

In the solid region:

$$\frac{\partial \varphi}{\partial \tau} = \frac{1}{\eta^2} \frac{\partial}{\partial \eta} \left(\eta^2 \frac{\partial \varphi}{\partial \eta} \right) \quad \chi(\tau) < \eta < 1, \quad \tau > \tau_f \quad (5b)$$

At the solid-liquid interface:

$$\frac{d\chi}{d\tau} = - \left. \frac{k_l}{k_s} \frac{\partial \varphi}{\partial \eta} \right|_{\eta=\chi^-} + \left. \frac{\partial \varphi}{\partial \eta} \right|_{\eta=\chi^+} \quad (6)$$

$$\varphi(\chi(\tau), \tau) = 0$$

Initial condition: $\varphi(\eta, \tau_f) = F(\eta) \quad 0 \leq \eta \leq 1$

Boundary conditions:

$$(1) \left. \frac{\partial \varphi}{\partial \eta} \right|_{\eta=0} = 0 \quad \tau > \tau_f$$

$$(2) - \left. \frac{\partial \varphi}{\partial \eta} \right|_{\eta=1} = \text{Bi}(\varphi - \varphi_\infty) \quad \tau > \tau_f$$

The time for the first stage τ_f and the temperature distribution function $F(\eta)$ are already known [7].

3.2 Numerical Calculation of the Solidification Stage

The melting problem of a slab of finite-thickness in a Cartesian coordinate system, with initial temperature below the freezing-point and subjected to a constant heat flux boundary condition (the second boundary condition) has been well solved using a variable time-step finite-difference method [8]. In the case of drop solidification in a tower, convective heat transfer takes place on the exterior surface of the drop (the third boundary condition) and the initial temperature is above the freezing-point. The difference equations here are

constructed using the finite control volume method, which has a clear physical sense. The numerical method is depicted briefly as follows.

As shown in Fig. 2, the drop radius is divided equally into N regions (control volumes) from the drop center to the exterior surface. The node point is located at the center of each region (method of internal point). At each step of the computation, e.g., at time τ , the interface is located at the $(i + 1)^{\text{th}}$ nodal point whose temperature is equal to the freezing point and the phase state is solid. At this time the temperature of each nodal point both in the solid region and in the liquid region is known. It is assumed that at time $\tau + \Delta\tau$, the interface moves from the $(i + 1)^{\text{th}}$ nodal point to the i^{th} nodal point. At time $\tau + \Delta\tau$, the fully implicit difference equation for the nodal points in the solid and liquid regions can be expressed as follows:

$$a_p \varphi_p = a_E \varphi_E + a_W \varphi_W + a_p^0 \varphi_p^0 \quad (7)$$

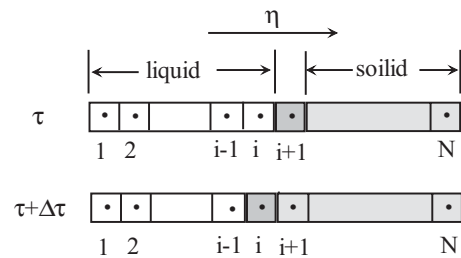


Figure 2. Nodal point division.

As shown in Fig. 3, the P nodal point denotes the point of discussion and the W, E points are the neighboring points of the P point. The point interfaces are denoted by w, e. In Eq. (7), the superscript 0 indicates the initial time τ , and $a_E = S_e / \Delta\eta$, $a_W = S_w / \Delta\eta$, $a_p = a_E + a_W + a_p^0$. In the solid region $a_p^0 = S_p \frac{\Delta\eta}{\Delta\tau}$, and in the liquid region $a_p^0 = S_p \frac{\Delta\eta}{\Delta\tau} \frac{\alpha_l}{\alpha_s}$, where S is the area factor, $S = 4\pi\eta^2$.

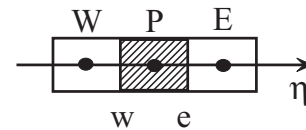


Figure 3. Schematic of the construction of the nodal point equation.

The difference equation of the interfacial nodal point i can be expressed as follows according to Eq. (6):

$$S_p \frac{\Delta\eta}{\Delta\tau} + S_p \left(\varphi_{i,f} - \frac{C_l}{C_s} \varphi_i^0 \right) \frac{\Delta\eta}{\Delta\tau} = \frac{k_l}{k_s} S_w \frac{\varphi_{i-1} - \varphi_{i,f}}{\Delta\eta} + S_e \frac{\varphi_{i+1} - \varphi_{i,f}}{\Delta\eta} \quad (8)$$

In Eq. (8), on the left hand side, the first term is the freezing heat of the i^{th} node; the second term is the energy change

due to the temperature change; on the right hand side, the first term and the second term are the heat transfer from the $(i - 1)^{\text{th}}$ and $(i + 1)^{\text{th}}$ nodal points to the i^{th} nodal point. $\varphi_{i,f}$ is the temperature of the freezing point, which equals zero. When $\Delta\tau$ is not an appropriate value, the residual value $\theta(\Delta\tau)$ between the left hand side and the right hand side of Eq. (8) is not equal to zero:

$$\theta(\Delta\tau) = S_p \frac{\Delta\eta}{\Delta\tau} + S_p \left(\varphi_{i,f} - \frac{C_l}{C_s} \varphi_i^0 \right) \frac{\Delta\eta}{\Delta\tau} - \frac{k_l}{k_s} S_w \frac{\varphi_{i-1} - \varphi_{i,f}}{\Delta\eta} - S_e \frac{\varphi_{i+1} - \varphi_{i,f}}{\Delta\eta} \quad (9)$$

An iteration procedure is used to get the appropriate value $\Delta\tau$ at each step so that $\theta(\Delta\tau) = 0$. At initial time τ , the temperatures of the nodal points in the solid region are known, and the boundary condition is also definite. At the next time $\tau + \Delta\tau$, the temperature of each point can be calculated using the tri-diagonal-matrix algorithm (TDMA). In the same way the temperature of each nodal point in the liquid region can be calculated. It is easy to find two time-step values $\Delta\tau_1$ and $\Delta\tau_2$ so that $\theta(\Delta\tau_1)$ and $\theta(\Delta\tau_2)$ are of opposite signs. The next guess for $\Delta\tau$ is obtained using linear interpolation:

$$\Delta\tau_{j+1} = \Delta\tau_j - \theta(\Delta\tau_j) \frac{\Delta\tau_j - \Delta\tau_{j-1}}{\theta(\Delta\tau_j) - \theta(\Delta\tau_{j-1})} \quad j = 3, 4, \dots \quad (10)$$

In all cases considered in this work, the above iteration procedure yields an accurate value ($|\theta(\Delta\tau)| < 10^{-6}$) for $\Delta\tau$ in about ten iterations. After calculating for the interfacial nodal point from the N^{th} nodal point to the first one, the whole calculation is finished.

4 Results and Discussion

4.1 Special Solidification Processes with the Initial Temperature at the Freezing-Point

In the case of drop solidification with an initial temperature at the freezing-point, the first stage presented above is not present. The second stage can be calculated directly with a grid number $N = 40$ (the grid number is taken to be 40 in all calculations performed in this work).

The Bi number is the thermal resistance ratio between the heat conduction within the drop and the convective heat transfer at the drop surface. In the water-cooling tower, the Bi number of a wax particle is relatively large, about 35–45. In the air-cooling tower, the Bi number of a urea particle is rather small, about 0.2–0.4. The solidification process has been modelled for different ranges of the Bi number. The position of the phase front versus the non-dimensional time with the cooling temperature $\varphi_\infty = -0.1$ is shown in Fig. 4. Fig. 4a is for a small Bi number and Fig. 4b is for a large Bi

number. A calculation result [5] from the literature is also shown in Fig. 4. It is shown that the two calculations agree except for a small deviation when the phase front is close to the sphere center. When the Bi number is relative small, the Bi number affects the non-dimensional time of the whole solidification process significantly, as shown in Fig. 4a. A small Bi number means that the resistance to heat transfer is mainly due to the convective heat transfer on the drop surface. Consequently, the convective heat transfer coefficient h affects drop solidification significantly. In the case of a large Bi number, the position of the phase front versus non-dimensional time profile does not change much with Bi number variation, especially when Bi is over 50, as shown in Fig. 4b. In this case, the third boundary condition is close to the first boundary condition, the heat transfer resistance is mostly within the drop, and a change in h causes little change to the solidification process.

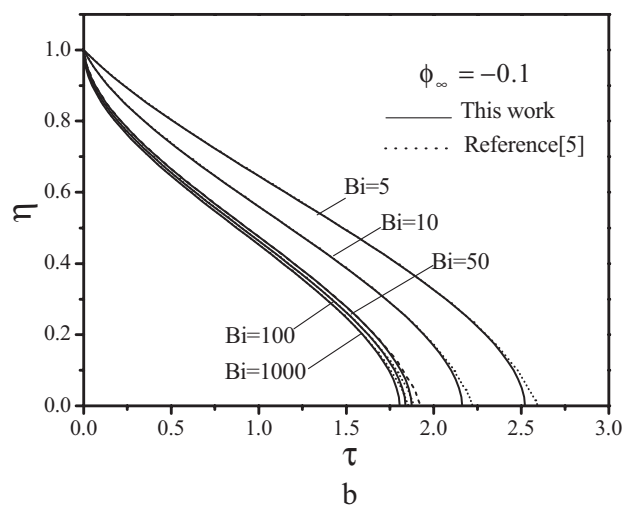
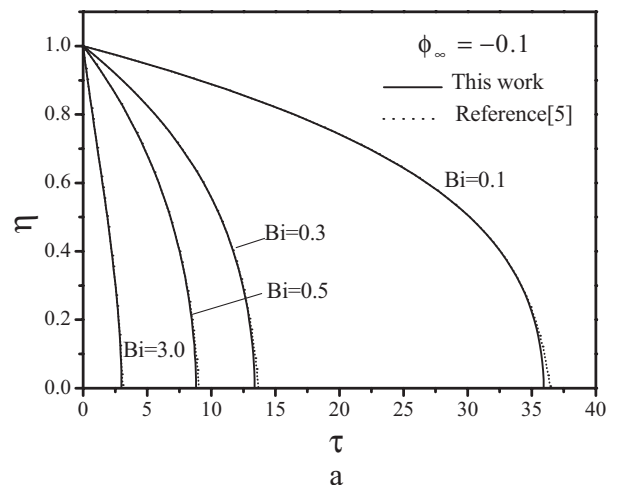


Figure 4. Non-dimensional phase front position vs. non-dimensional time.

4.2 A Simplified Calculation Method for an Initial Temperature above the Freezing Point

In a real industrial process, the temperature of the melted material is higher than the freezing-point. In the granulation process for 58[#] wax (the freezing point is in the range of 58–60 °C), the temperature of the melted wax is about 70 °C. In the urea granulation process, the temperature of the melted urea is about 140 °C (the freezing point of urea is about 132.7 °C). In the following two cases, the time for the first stage is very short relative to the second stage. The ratio between the time for the first stage and the time for the second stage is about 1/200 when the Bi number is about 40 and about 1/50 when the Bi number is about 0.3. Therefore, the numerical calculation is performed from the Nth nodal point directly, using the initial condition of the first stage to simplify the calculation. In this way, when the Nth nodal point calculation is completed, a time step $\Delta\tau_i$ is obtained, which includes the time for the first stage τ_f and the time for freezing the Nth nodal point.

5 Analysis of the Solidification in Wax and Urea Granulation

Two typical solidification processes – wax granulation in a water-cooling tower and urea granulation in an air-cooling tower – are analyzed. The physical parameters of 58[#] wax and urea used in this paper are listed in Tab. 1.

5.1 Solidification of a Wax Drop in a Water-Cooling Tower

Wax particles produced in a water-cooling tower have a spherical shape and uniform diameter of 4–5 mm, which is one of the merits of this new technology. In the case of 58[#] wax granulation, particles with diameters of 4 mm and 5 mm are taken as calculation examples. It is assumed that the initial temperature of the drop is 70 °C and the temperature of the cooling water is 43 °C [1]. The related data on particle movement and heat transfer are listed in Tab. 2.

Fig. 5 shows the phase front position in the wax drop versus time for different drop sizes. The phase front in the drop moves from the drop surface towards the drop center. In the solidification process, the velocity of the moving phase front is faster at the beginning and at the end than in the middle, like an “S” pattern. At the beginning, due to the large Bi

Table 2. Parameters related to movement and heat transfer of 58[#] wax particle in a water cooling tower.

Diameter, mm	Terminal velocity, m/s	Nu number	Bi number
4.0	0.13	38.4	37.8
5.0	0.15	45.8	45.0

number, the surface temperature of the drop decreases quickly; when the phase front is close to the center, the area of the phase front becomes much smaller, so the velocity of the moving phase front becomes high again. The influence of the drop radius R on solidification comes from the definition of the Bi number and non-dimensional time τ . In the wax granulation process, h has little effect on the solidification of the wax drop because of the large Bi number. From the definition of τ , the real time needed for solidification with a large Bi number has the approximate relation with particle radius R, $\tau \propto 8 R^2$. As shown in Fig. 5, the non-dimensional times for the solidification of 4 mm and 5 mm drops are almost the same, about 1.1 but the real times are 27.9 s and 43.6 s, respectively. If wax drops need to be solidified in the tower, the necessary height of the towers for 4 mm and 5 mm particles are 3.6 m and 6.5 m, respectively, which evidently is not optimal.

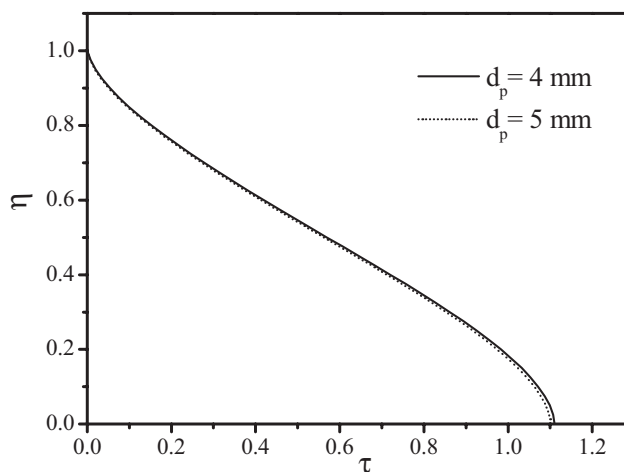


Figure 5. Non-dimensional phase front position vs. non-dimensional time for wax particles of different diameters.

The temperature of the cooling medium is another important factor affecting the solidification process. Fig. 6 shows the solidification process of a $d_p = 4.5$ mm particle with an initial temperature $T_o = 70$ °C at different temperatures of the cooling medium. The lower the temperature of the cooling medium, the less time the solidification needs. However, the decreasing trend lessens as the cooling temperature decreases.

Table 1. Physical parameters of 58[#] wax and urea.

Substance	Average density, kg/m ³	Heat capacity, J/(kg K)		Thermal conductivity, W/(m K)		Latent heat, J/kg
		Solid	Liquid	Solid	Liquid	
58 [#] wax	840	2462	3056	0.326	0.287	$1.953 \cdot 10^5$
Urea	1333	1917	2012	0.725	0.413	$2.463 \cdot 10^5$

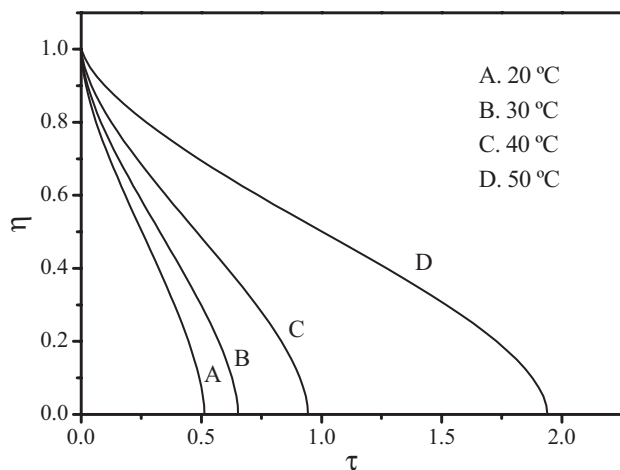


Figure 6. Non-dimensional phase front position vs. non-dimensional time for wax particles in different cooling temperatures.

The non-dimensional temperature distributions in the drop at different times are shown in Fig. 7. This result is calculated for $d_p = 4.5$ mm, temperature of the cooling medium $T_\infty = 43$ °C and initial temperature of the wax drop $T_o = 70$ °C. It can be seen that there is a turning point in each curve of temperature distribution in Fig. 7. At this point, the temperature gradient is discontinuous as also expressed in Eq. (6). This point corresponds to the location of the phase front, at which point the temperature is zero. The surface temperature (where $\eta = 1$) approaches the temperature of the cooling medium quickly because of the large Bi number.

In wax granulation, the residence time of the drop in the water-cooling tower depends on the height of the tower. If the temperature of the cooling water is not low enough the wax drop cannot be fully solidified, causing wax particles to stick to each other easily. In this case, granulation cannot be operated stably. If the temperature of the cooling medium is too low, although the particles can be fully solidified, the water temperature in the granulation hole at the bottom of the tower is difficult to maintain, but this temperature is the key point for stable drop formation. The energy consumption will increase and abnormal operations tend to happen, such as wax blocking in the nozzles. In order to decrease the energy consumption, the temperature of the cooling water in the tower should be raised to suppress the natural convective heat transfer between the hot water in the granulation hole and the cooling water in the tower. The higher the temperature of the cooling water, the higher is the height of the tower needed. However, both the high temperature of the cooling water and high height of the tower are not optimal designs. Therefore, a two-stage cooling is designed for the solidification of the wax drop. The first stage cooling enables the drop to form a solid shell in the tower, preventing the particles from stick-

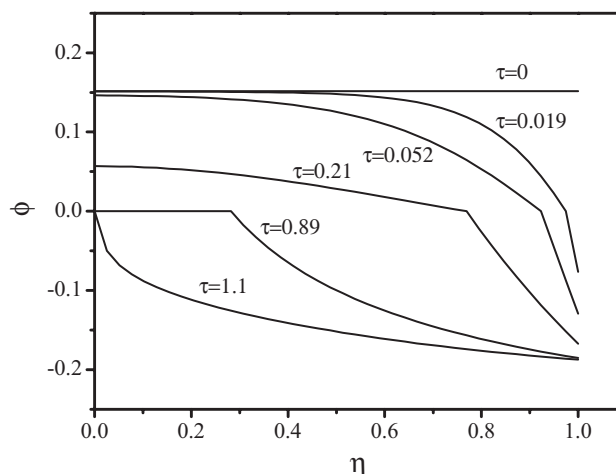


Figure 7. Temperature distribution within the wax particle at different times.

ing to each other in the tower and during discharge process. After the particles flow out of the tower, the second stage cooling is performed in a chute by spraying cooling water on the particles.

Therefore, the temperature of the cooling water should be optimized for stable granulation and minimization of the energy consumption. The prerequisite condition for stable granulation is that the wax drops should be cooled enough before they flow out of the tower. Experiments showed that the temperature of the cooling water should be in the range 40–45 °C, at which temperature granulation for 58[#] wax can be stably performed in a laboratory granulator with a capacity of ~55–60 kg/h and a height of 1200 mm.

5.2 Solidification of Urea Drops in an Air-Cooling Tower

In urea granulation, melted urea is sprayed into the tower by a sprayer. The average drop diameter is about 1.5 mm. The solidification of the urea drop is analyzed for drop diameters of 1.0, 1.5, and 2.0 mm. It is assumed that the average rising velocity of the air in the tower is 1.5 m/s, the average air temperature is 40 °C and the temperature of the melted urea is 140 °C. Under these conditions, the particle settling velocity, Nu number and Bi number are listed in Tab. 3.

The position of the phase front in the urea drop versus non-dimensional time for the different particle sizes is shown in Fig. 8. The three curves in Fig. 8 are not close to each other, unlike the curves in Fig. 5. The Bi number is small, in

Table 3. Parameters related to movement and heat transfer of urea particles in an air-cooling tower.

Diameter, mm	Terminal velocity relative to the air, m/s	Absolute terminal velocity, m/s	Nu number	Bi number
1.0	5.0	3.5	12.5	0.238
1.5	7.3	5.8	17.6	0.334
2.0	8.4	6.9	21.3	0.405

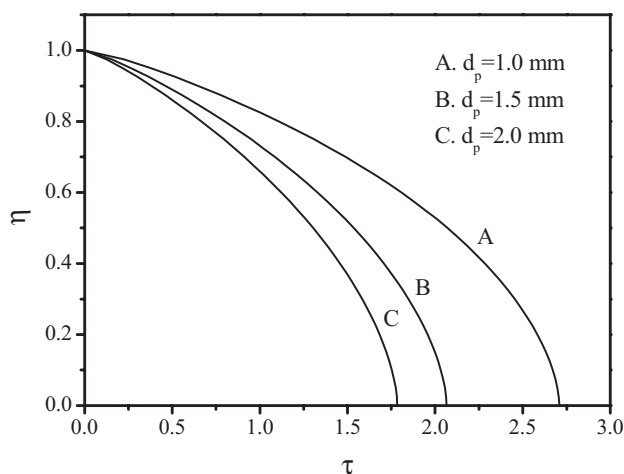


Figure 8. Non-dimensional phase front position vs. non-dimensional time for urea particles of different diameters.

the range of 0.2–0.4. The thermal resistance of the convective heat transfer from the drop surface and the thermal resistance of the heat conduction in the drop affect the solidification simultaneously. According to the definition of τ , we have $\tau \propto \tau R^2$ and the real solidification times of the three size particles are 2.4, 4.1, and 6.3 s, respectively. By multiplying their settling velocity, the necessary heights of the tower for the solidification of the urea drop are 8.4, 23.7, and 43.4 m, respectively. It is also shown that the necessary height of the air-cooling tower clearly depends on the particle size.

For a urea particle diameter $d_p = 1.5$ mm, temperature of the melted urea of 140°C and temperatures of the cooling air in the tower of 30°C , 40°C , and 50°C , respectively, the positions of the phase front versus non-dimensional time are shown in Fig. 9. The real times of solidification at these three different temperatures of cooling media are 3.7, 4.1, and 4.5 s and the heights of the tower needed for the solidification of the urea drop are 21.7, 23.7, and 26.2 m, respectively.

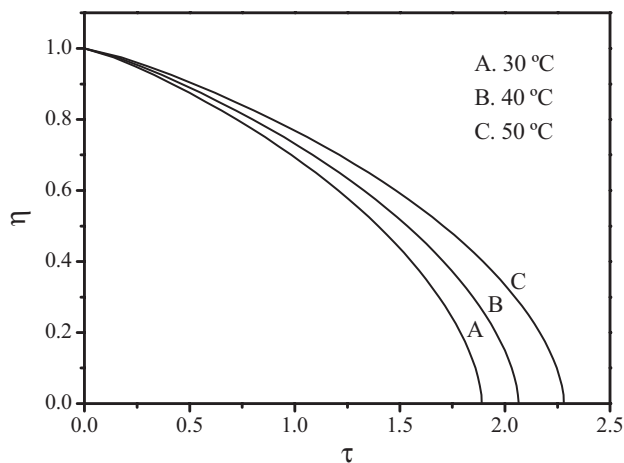


Figure 9. Non-dimensional phase front position vs. non-dimensional time for urea particles in different cooling temperatures.

Additionally, the temperature of the urea particles should be decreased to about 50°C , so the height of the air-cooling tower is usually taken to be above 60 m.

The temperature distributions within a particle of $d_p = 1.5$ mm solidified in cooling air at 40°C at different times are shown in Fig. 10. Similar to the temperature distribution of the wax particles in Fig. 7, there is also a turning point in each curve, which corresponds to the phase front. The surface temperature decreases slowly because of the small convective heat transfer coefficient h . Fig. 10 also shows that the temperature in the liquid region approaches the freezing-point in a short time due to the temperature of the phase front and initial temperature of the drop, which is close to the freezing-point.

6 Conclusions

Solidification of a melted drop in an immiscible cooling medium is analyzed, and a physical model for the cooling and solidification of the drop is established. The movement of the phase front and the temperature distribution in the drop are calculated. The influences of the key factors in drop solidification, such as the drop size, temperature of the cooling medium and convective heat transfer coefficient, are analyzed. Two cases of drop cooling and solidification of industrial interest are calculated, namely wax granulation in a water-cooling tower and urea granulation in an air-cooling tower. The cooling medium affects the heat transfer significantly. When the cooling medium is water, the heat transfer resistance is mainly within the particle. When the cooling medium is air, the heat transfer resistance is in the cooling medium and within the particle, both of which influence the solidification process. The characteristics of the heat transfer between the particle and the cooling medium have a significant influence on the tower height. The solidification model and numerical calculation results can be used as the basis for tower height design and temperature setting of the cooling medium.

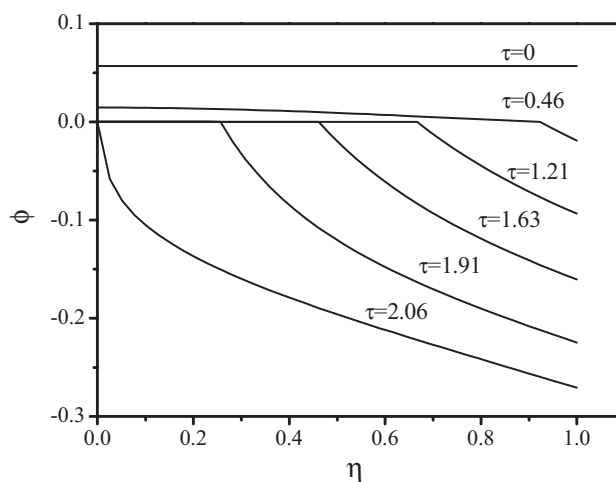


Figure 10. Temperature distribution within urea particles at different times.

Acknowledgments

The authors wish to express their appreciation for the financial support of this study by China National Petroleum Corporation (CNPC) Innovation Fund, grant number No. 03E7039.

Received: October 30, 2004 [CET 7093]

Symbols used

A_p	[m ²]	particle projecting area in moving direction
a	[-]	coefficient in the difference equation
Bi	[-]	Bi number
b	[-]	correlation coefficient
C	[J/kg K]	heat capacity
d	[m]	particle(drop) diameter
F_B	[N]	buoyancy force
F_D	[N]	drag force
F_g	[N]	gravity
g	[m/s ²]	gravity acceleration
h	[W/m ² K]	convective heat transfer coefficient
k	[W/m K]	thermal conductivity
L	[J/kg]	latent heat of phase change
N	[-]	grid number
Nu	[-]	Nu number
Pr	[-]	Pr number
R	[m]	particle (drop) radius
Re	[-]	Re number
r	[m]	spherical coordinate direction
S	[-]	factor of area
T	[°C]	temperature
t	[s]	time
u_t	[m/s]	terminal velocity of the particle (drop)
X	[m]	phase front position
α	[m ² /s]	thermal diffusivity
Δ	[-]	step length
φ	[-]	non-dimensional temperature
τ	[-]	non-dimensional time

η	[-]	non-dimensional spherical coordinate direction
θ	[-]	residual value function
χ	[-]	non-dimensional phase front position
φ_0	[-]	non-dimensional initial temperature
φ_∞	[-]	non-dimensional cooling temperature
μ	[kg/m s]	viscosity
ξ	[-]	drag coefficient
ρ	[kg/m ³]	density

Subscripts

c	continuous phase
d	dispersed phase
f	freezing
i	nodal point order number
j	iteration number
l	liquid
s	solid
W, P, E	nodal point label
w, e	interface of nodal point

Superscripts

0	initial time
-----	--------------

References

- [1] J.-Y. Fang, Y.-Z. Xi, T.-J. Wang, Y. Jin, *Chem. Eng. Tech.* **2004**, 27 (9), 1039. DOI: 10.1002/ceat.200402036
- [2] J. Crank, *Free and Moving Boundary Problems*, Clarendon Press, Oxford **1987**.
- [3] S V. Patankar, *Numerical Heat Transfer and Fluid Flow*, Hemisphere Pub. Co., Washington **1980**.
- [4] R. H. Perry, D. W. Green, J. O. Maloney, *Perry's Chemical Engineers' Handbook*, 7th ed., McGraw-Hill, New York **1997**, pp6–51.
- [5] H. Zhang, Y.-Y. Wang, Y.-Z. Wu, *Journal of Xi'an Jiaotong University* **1995**, 29 (11), 71.
- [6] P. N. Rowe, K. T. Claxton, *Trans. Inst. Chem. Eng.* **1965**, 43, T321.
- [7] H. S. Carslaw, J. C. Jaeger, *Conduction of Heat in Solids*, Clarendon Press, Oxford **1986**.
- [8] W. W. Yuen, A. M. Kleinman, *AIChE J.* **1980**, 26 (5), 828.